Journal of Zhejiang University-SCIENCE B (Biomedicine & Biotechnology)
ISSN 1673-1581 (Print); ISSN 1862-1783 (Online)
www.zju.edu.cn/jzus; www.springerlink.com
E-mail: jzus@zju.edu.cn

# Electromagnetic effects on the biological tissue surrounding a transcutaneous transformer for an artificial anal sphincter system*

Peng ZAN†[1], Bang-hua YANG[1], Yong SHAO[1], Guo-zheng YAN[2], Hua LIU[2]

([1]*Shanghai Key Laboratory of Power Station Automation Technology, College of Mechatronics Engineering and Automation, Shanghai University, Shanghai 200072, China*)

([2]*School of Electronics, Information and Electrical Engineering, Shanghai Jiao Tong University, Shanghai 200240, China*)

†E-mail: zanpeng@shu.edu.cn

Received Feb. 22, 2010; Revision accepted July 1, 2010; Crosschecked Aug. 10, 2010

**Abstract:** This paper reports on the electromagnetic effects on the biological tissue surrounding a transcutaneous transformer for an artificial anal sphincter. The coupling coils and human tissues, including the skin, fat, muscle, liver, and blood, were considered. Specific absorption rate (SAR) and current density were analyzed by a finite-length solenoid model. First, SAR and current density as a function of frequency (10–$10^7$ Hz) for an emission current of 1.5 A were calculated under different tissue thickness. Then relations between SAR, current density, and five types of tissues under each frequency were deduced. As a result, both the SAR and current density were below the basic restrictions of the International Commission on Non-Ionizing Radiation Protection (ICNIRP). The results show that the analysis of these data is very important for developing the artificial anal sphincter system.

**Key words:** Artificial anal sphincter, Transcutaneous energy transmission, Current density, Specific absorption rate
**doi:**10.1631/jzus.B1000058 **Document code:** A **CLC number:** R318.6

## 1 Introduction

There have been many types of artificial anal sphincters developed to control anal incontinence (Lehur *et al*., 2000; Guralnick and Webster, 2003; Kakubari *et al*., 2003; Finlay *et al*., 2004; Doll *et al*., 2007; Zan *et al*., 2008a), but to date these devices have been associated with many complications and have not gained acceptance. To overcome the shortcomings, a transcutaneous power delivery system (TPDS) is applied externally to the totally implantable artificial anal sphincter (Zan *et al*., 2008b; 2009). This method is superior to others because it reduces the possibility of infection and keeps the skin uninjured, and also provides the patient with a better quality of life.

The TPDS transfers energy by means of electromagnetic induction between two transcutaneous coils placed face-to-face on each side of the lateral abdominal skin. However, for the practical application of this method, it is necessary to investigate the electromagnetic effect of the TPDS on biological tissue.

Specific absorption rate (SAR) and current density are usually used as indexes of biological electromagnetic safety (Sullivan *et al*., 1987). A mathematical method derived from Cristina and Parise (2008)'s research allows for the rapid and accurate computation of the SAR induced inside a plane geometry fat-muscle tissue by exposure to a shortwave diathermy induction coil. However, the current density was not considered and the types of biological tissues were only limited to fat and muscle. Shiba *et al*. (2008) analyzed the SAR and current density with an electromagnetic simulator in a model consisting of a primary coil and a human trunk including the skin, fat,

* Project supported by the National Natural Science Foundation of China (No. 60975079), the Scientific Special Research Fund for Training Excellent Young Teachers in Higher Education Institutions of Shanghai (No. shu10052), the Innovation Fund of Shanghai University, and the '11th Five-Year Plan' 211 Construction Project of Shanghai University, China

muscle, small intestine, backbone, and blood. However, the position and shape of the coils in TPDS are different from the ones in Shiba *et al*. (2008), so the analytic model and related biological tissues need to be reconsidered for the artificial anal sphincter system (AASS).

Generally, there have not been any studies on the electromagnetic effects on biological tissue surrounding a transcutaneous transformer for an artificial anal sphincter. In this paper, according to the basic restrictions defined by the International Commission on Non-Ionizing Radiation Protection (ICNIRP Guideline, 1998), both the SAR and current density are analyzed by a finite-length solenoid model. At the same time, the coupling coils and human tissues including the skin, fat, muscle, liver, and blood are considered for the AASS.

## 2 Materials and methods

### 2.1 Transcutaneous power delivery system

An artificial anal sphincter with a TPDS consists of a sensor and execution unit, an internal control unit, an external control unit, an external energy emitting unit, and two transmitting coils. As Fig. 1 shows, the whole system is composed of two components. One is implanted inside the body; the other is placed outside the body. The whole implanted part is powered by the TPDS.

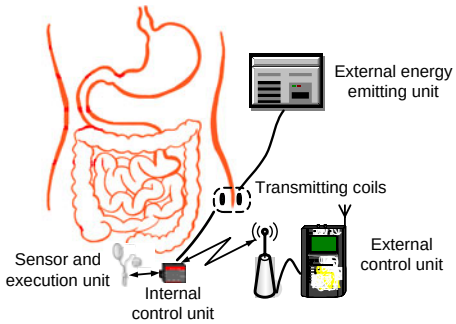


**Fig. 1 Artificial anal sphincter system architecture**

An equivalent circuit of the TPDS is shown in Fig. 2a. In the TPDS, the energy receiver gets the energy from the coupling between the primary and the secondary coils. Fig. 2b shows the transcutaneous transformer considered in this paper. The external coil has an outside diameter of 30 mm (78 turns), inside diameter of 10 mm, and thickness of 5 mm. The internal coil has an outside diameter of 35 mm (154 turns), inside diameter of 12 mm, and thickness of 5 mm. The coils are made of copper litz-wire, in consideration of the skin effect, which has the tendency for high-frequency current to flow on the surface of a conductor. A maximum power of 300 mW in the TPDS is required to power the artificial anal sphincter.

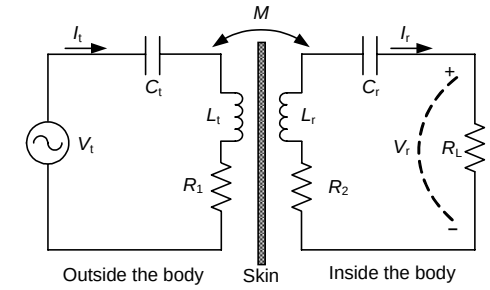


$V_t$: input voltage
$V_r$: output voltage
$I_t$: input current
$I_r$: output current
$C_t$ and $C_r$: resonant capacitances
$M$: mutual inductance
$L_t$: inductances of the emitting coil
$L_r$: inductances of the receiving coil
$R_1$: primary coil resistance
$R_2$: secondary coil resistance
$R_L$: load for the artificial anal sphincter

(a)

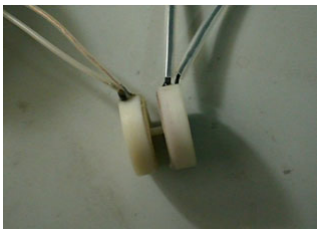

(b)

**Fig. 2 An equivalent circuit of the transcutaneous power delivery system (TPDS) (a) and the transcutaneous transformer (b)**

### 2.2 SAR and current density

SAR and current density are used as two most important indexes for electromagnetic influences, which can be expressed by

$$\mathrm{SAR} = \sigma |E|^2 / (2\rho), \tag{1}$$

$$J = \sigma |E|, \tag{2}$$

where $E$ is the electromotive intensity, $\sigma$ is the electrical conductivity of biological tissue, $\rho$ is the density of biological tissue, and $J$ is the current density. As defined by the ICNIRP (2009), Table 1 shows the basic restrictions on the SAR and current density.

**Table 1 ICNIRP's basic restrictions for time-varying electric and magnetic fields***

| Frequency range (Hz) | Current density for head and trunk (mA/m$^2$) | Whole-body average SAR (W/kg) | Localized SAR for head and trunk (W/kg) | Localized SAR for limbs (W/kg) |
|---|---|---|---|---|
| $10^3$–$10^5$ | $f_e$/100 | – | – | – |
| $10^5$–$10^7$ | $f_e$/100 | 0.4 | 10 | 20 |

* Adopted from ICNIRP (2009). $f_e$: emitting frequency (Hz)

### 2.3 Finite-length solenoid model

Because both of the transcutaneous coils are placed face-to-face on each side of the lateral abdominal skin, and the current in the first coil is far larger than the current in the second coil, we can ignore the electromagnetic influence generated by the second coil. A finite-length solenoid model for numerical analysis is shown in Fig. 3 (Arai *et al*., 2002; Tai and Liao, 2007).

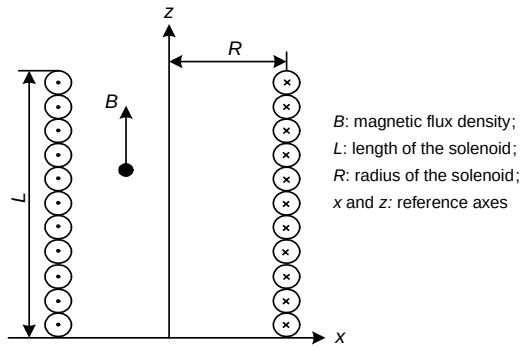


**Fig. 3 Finite-length solenoid model for numerical analysis**
Adopted from Arai *et al*. (2002) and Tai and Liao (2007)

According to the Maxwell's law, magnetic flux density $B$ and electromotive intensity $E$ can be expressed by

$$B=\frac{2\pi Rn^2\mu_0 I}{\sqrt{(2\pi Rn)^2+1}}, \tag{3}$$

$$I=I_0 e^{-j\omega t}, \tag{4}$$

$$E=-j\omega I_0\cdot\frac{x\pi Rn^2\sqrt{\mu_0\varepsilon_0}}{\sqrt{(2\pi Rn)^2+1}}\cdot e^{-j\omega t}, \tag{5}$$

where $n$ is the turn number of the solenoid, $\mu_0$ is the vacuum permeability, $I$ is the low-frequency current and $I_0$ is the virtual value of $I$, $\omega$ is the angular frequency, $t$ is the time, $j$ is the imaginary unit, and $\varepsilon_0$ is the relative permittivity.

Using Eqs. (1)–(5), SAR and current density can be expressed as follows:

$$\mathrm{SAR}=\frac{\sigma}{\rho}\left(\frac{\omega I_0 x\pi Rn^2\sqrt{\mu_0\varepsilon_0}}{\sqrt{(2\pi Rn)^2+1}}\right)^2, \tag{6}$$

$$J=\frac{\sigma\omega I_0 x\pi Rn^2\sqrt{\mu_0\varepsilon_0}}{\sqrt{(2\pi Rn)^2+1}}. \tag{7}$$

According to different frequencies and tissues, the electromagnetic effects can be analyzed by the solenoid model. The relation between the conductivity and frequency is shown in Fig. 4 (Gabriel S. *et al*., 1996; Zhao *et al*., 2004; Gabriel C. *et al*., 2009).

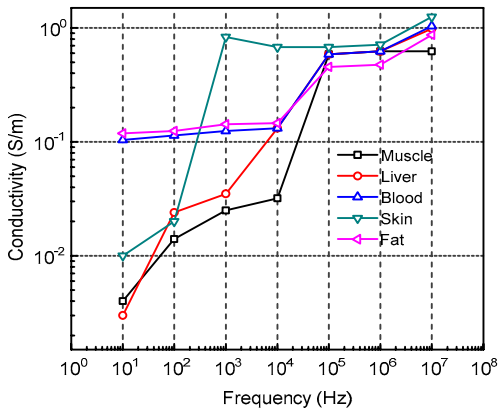


**Fig. 4 Relation between conductivity and frequency of the solenoid model**
Adopted from Gabriel S. *et al*. (1996), Zhao *et al*. (2004), and Gabriel C. *et al*. (2009)

## 3 Results and discussion

The simulation parameters for electromagnetic effects on biological tissues are listed in Table 2.

Using Eqs. (6) and (7), the SAR and current density of the muscle (as a typical value) can be calculated under each frequency and tissue thickness.

**Table 2 Simulation parameters for electromagnetic effects on biological tissues**

| Parameter | Value |
|---|---|
| Thickness of biological tissue, $d_0$ (mm) | 0 5 10 15 20 25 30 |
| Working frequency, $f_w$ (Hz) | 10 $10^2$ $10^3$ $10^4$ $10^5$ $10^6$ $10^7$ |
| Effective current, $I_0$ (A) | 1.5 |
| Average density of biological tissue, $\rho$ (kg/m$^3$) | 1000 |
| Receiving power (mW) | 300 |
| Load impedance (Ω) | 30 |

As Fig. 5a shows, the SAR of the muscle becomes larger as the frequency and the tissue thickness rise, and the thickness influences the SAR less than the frequency does. The maximum SAR value of the human trunk is 0.0103 W/kg under $10^7$ Hz, which is much smaller than the ICNIRP's basic restrictions of the SAR for the head and trunk (10 W/kg) and the whole-body average (0.4 W/kg).

As Fig. 5b shows, the current density of the muscle also becomes larger as the frequency and the tissue thickness rise. The thickness also influences the current density less than the frequency does. As the frequency rises upon $10^6$ Hz, the current density becomes obviously larger. The maximum current density 5005.8 mA/m$^2$ under $10^7$ Hz is sufficiently smaller than the ICNIRP's basic restrictions of $10^5$ mA/m$^2$.

The SAR and current density of five types of tissues under each frequency are calculated (Fig. 6). Each tissue produces a different SAR and current density, because each tissue has a different specific conductivity. At the same time, the maximum SAR and current density appear in muscle due to its higher conductivity.

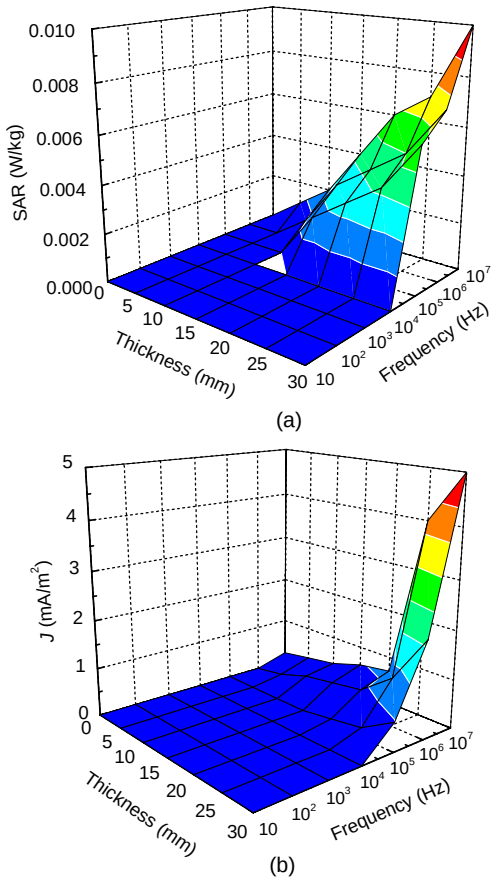


**Fig. 5 Specific absorption rate (SAR) (a) and current density ($J$) (b) of the muscle calculated according to frequency and tissue thickness**

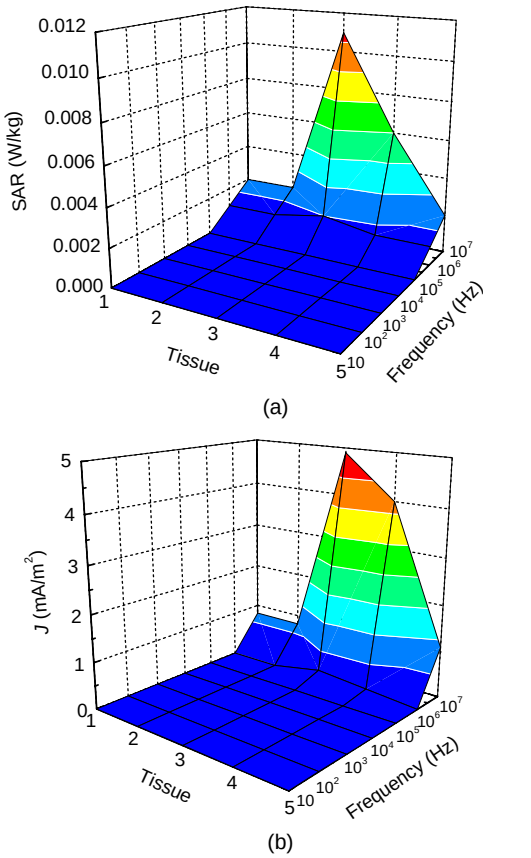


**Fig. 6 Specific absorption rate (SAR) (a) and current density ($J$) (b) of five types of tissues under frequencies of 10–$10^7$ Hz**

Tissue: 1, skin; 2, fat; 3, muscle; 4, blood; 5, liver

The transmission frequency of the TPDS developed in this paper is 29800 Hz, and the effective value of the emitting current is about 1.5 A. The SAR and current density of different types of biological tissues can be calculated under the precondition (Fig. 7). The SAR and current density are sufficiently small and far below the ICNIRP's basic restrictions.

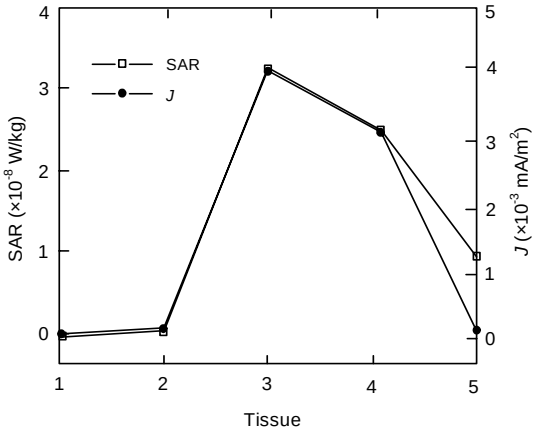


**Fig. 7 Specific absorption rate (SAR) and current density of different types of tissues under the transmission frequency of 29800 Hz**
Tissue: 1, skin; 2, fat; 3, muscle; 4, blood; 5, liver

## 4 Conclusions

We analyzed SAR and current density in biological tissues surrounding a transcutaneous transformer. First, a finite-length solenoid model for numerical analysis was built. SAR and the current density under frequencies of 10–$10^7$ Hz were calculated, and human tissues including the skin, fat, muscle, liver, and blood were considered. We found that the SAR and the current density in the vicinity of the transformer were sufficiently small for a transcutaneous transmission of 300 mW and 1.5 A.

The result shows that taking into account the biological tissue is very important for developing the transcutaneous transformer, not only for the artificial anal sphincter, but also for other implanted devices with the TPDS. In the future, further animal experiments will be undertaken and evaluated for developing the safety and performance of the TPDS.

## References

Arai, K., Ninomiya, A., Ishigohka, T., Takano, K., Matsui, K., Michael, P.C., Vieira, R.F., Martovetsky, N.N., Kaiho, K., Nakajima, H., *et al*., 2002. Acoustic emission during DC operations of the ITER central solenoid model coil. *IEEE Trans. Appl. Supercon.*, **12**(1):504-507. [doi:10.1109/TASC.2002.1018453]

Cristina, S., Parise, M., 2008. Calculation of EM Power Deposition for Exposure to Shortwave Induction Diathermy. IET 7th International Conference on Computation in Electromagnetics. Brighton, UK, p.208-209. [doi:10.1049/cp:20080264]

Doll, A.F., Wischke, M., Geipel, A., Goldschmidtboeing, F., Ruthmann, O., Hopt, U.T., Schrag, H., Woias, P., 2007. A novel artificial sphincter prosthesis driven by a four-membrane silicon micropump. *Sensor. Actuat. A: Phys.*, **139**(1-2):203-209. [doi:10.1016/j.sna.2007.03.025]

Finlay, G., Richardson, W., Hajivassiliou, C.A., 2004. Outcome after implantation of a novel prosthetic anal sphincter in humans. *Br. J. Surg.*, **91**(11):1485-1492. [doi:10.1002/bjs.4721]

Gabriel, C., Peyman, A., Grant, E.H., 2009. Electrical conductivity of tissue at frequencies below 1 MHz. *Phys. Med. Biol.*, **54**(16):4863-4878. [doi:10.1088/0031-9155/54/16/002]

Gabriel, S., Lau, R.W., Gabriel, C., 1996. The dielectric properties of biological tissues: III. Parametric models for the dielectric spectrum of tissues. *Phys. Med. Biol.*, **41**(11):2271-2293. [doi:10.1088/0031-9155/41/11/003]

Guralnick, M.L., Webster, G.D., 2003. Transcorporal insertion of AMS800 artificial urinary sphincter. *Atlas Urol. Clin.*, **11**(1):83-87. [doi:10.1016/S1063-5777(02)00067-1]

ICNIRP Guideline, 1998. Guidelines for limiting exposure to time-varying electric, magnetic, and electromagnetic fields (up to 300 GHz). *Health Phys.*, **74**(4):494-522.

ICNIRP, 2009. Exposure to High Frequency Electromagnetic Fields, Biological Effects and Health Consequences (100 kHz–300 GHz). Available from http://www.icnirp.de/activities.htm [Accessed on Jan. 2, 2010]

Kakubari, Y., Sato, F., Matsuki, H., Sato, T., Luo, Y., Takagi, T., Yambe, T., Nitta, S., 2003. Temperature control of SMA artificial anal sphincter. *IEEE Trans. Magn.*, **39**(5):3384-3386. [doi:10.1109/TMAG.2003.816158]

Lehur, P.A., Roig, J.V., Duinslaeger, M., 2000. Artificial anal sphincter: prospective clinical and manometric evaluation. *Dis. Colon Rectum*, **43**(8):1100-1106. [doi:10.1007/BF02236557]

Shiba, K., Nagato, T., Tsuji, T., Koshiji, K., 2008. Energy transmission transformer for a wireless capsule endoscope: analysis of specific absorption rate and current density in biological tissue. *IEEE Trans. Biomed. Eng.*, **55**(7):1864-1871. [doi:10.1109/TBME.2008.919721]

Sullivan, D.M., Borup, D.T., Gandhi, O.P., 1987. Use of the finite-difference time-domain method in calculating EM

absorption in human tissues. *IEEE Trans. Biomed. Eng.*, **34**(2):148-157. [doi:10.1109/TBME.1987.326039]

Tai, C.M., Liao, C.N., 2007. A physical model of solenoid inductors on silicon substrates. *IEEE Trans. Microw. Theory Tech.*, **55**(12):2579-2585. [doi:10.1109/TMTT.2007.910069]

Zan, P., Yan, G.Z., Liu, H., 2008a. A novel artificial anal sphincter system based on transcutaneous energy transmission. *High Technol. Lett.*, **14**(4):423-428. [doi:10.3772/j.issn.1006-6748.2008.04.016]

Zan, P., Yan, G.Z., Liu, H., 2008b. Modeling of human colonic blood flow for a novel artificial anal sphincter system. *J. Zhejiang Univ.-Sci. B*, **9**(9):734-738. [doi:10.1631/jzus.B0820099]

Zan, P., Yan, G.Z., Liu, H., Luo, N., Zhao, Y., 2009. Adaptive transcutaneous power delivery for an artificial anal sphincter system. *J. Med. Eng. Technol.*, **33**(2):136-141. [doi:10.1080/03091900801943205]

Zhao, X.L., Kinouchi, Y., Yasuno, E., Gao, D., Iritani, T., Morimoto, T., Takeuchi, M., 2004. A new method for noninvasive measurement of multilayer tissue conductivity and structure using divided electrodes. *IEEE Trans. Biomed. Eng.*, **51**(2):362-370. [doi:10.1109/TBME.2003.820403]